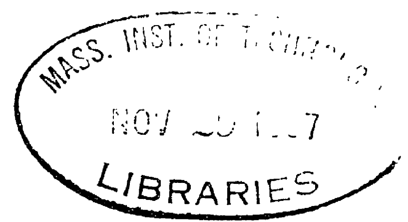

MASS. INST. OF TECHNOLOGY
NOV 1967
LIBRARIES

A PLANAR GERMANIUM THERMOPHOTOVOLTAIC ENERGY CONVERTER

by

JOHN GABRIEL KASSAKIAN

S.B., Massachusetts Institute of Technology

(1965)

SUBMITTED IN PARTIAL FULFILLMENT OF THE

REQUIREMENTS FOR THE DEGREES OF

MASTER OF SCIENCE

and

ELECTRICAL ENGINEER

at the

MASSACHUSETTS INSTITUTE OF TECHNOLOGY

September, 1967

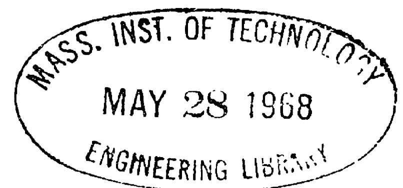

MASS. INST. OF TECHNOLOGY
MAY 28 1968
ENGINEERING LIBRARY

Signature of Author ______________________________
Department of Electrical Engineering, September 6, 1967

Certified by ______________________________
Thesis Supervisor

Accepted by ______________________________
Chairman, Departmental Committee on Graduate Students

A PLANAR GERMANIUM THERMOPHOTOVOLTAIC ENERGY CONVERTER

by

JOHN GABRIEL KASSAKIAN

Submitted to the Department of Electrical Engineering on September 6, 1967 in partial fulfillment of the requirements for the degrees of Master of Science and Electrical Engineer.

ABSTRACT

The structural advantages of a planar p-i-n photovoltaic cell in which both junctions are formed on the same face of an intrinsic region are discussed. Device parameters are reviewed and a specific design is proposed. Fabrication techniques are discussed.

Several diodes are fabricated and tested in a probing machine. Series resistance effects due to the bulk material are observed at low injection levels. Series resistance due to the contact and finger structure is evident at high level operation. An open circuit voltage of 60 mv is obtained illuminating the back side of the device with a microscope light.

Problems associated with the fabrication of a complete TPV device are anticipated and solutions to these problems are proposed.

Thesis Supervisor: Bruce D. Wedlock

Title: Associate Professor of Electrical Engineering

ACKNOWLEDGEMENTS

The author wishes to acknowledge with appreciation the help and encouragement of his thesis supervisor, Professor Bruce D. Wedlock. He also wishes to thank Professors Paul E. Gray, Richard B. Adler, David H. Navon, and Robert H. Rediker for their many helpful discussions. Finally the author offers heartfelt thanks to WMR for moral support and encouragement during times of experimental crises.

This work was made possible by support from the U.S. Army Electronics Command under contract no. DA-28-043-AMC-01978(E).

TABLE OF CONTENTS

		Page
ABSTRACT		1
ACKNOWLEDGEMENTS		2
TABLE OF CONTENTS		3
LIST OF ILLUSTRATIONS		4
CHAPTER I	INTRODUCTION	5
CHAPTER II	THE PLANAR p-i-n THERMOPHOTOVOLTAIC CELL	9
	Optimum Parameters for a Planar Device	13
	Analog Evaluation of Series Resistance	17
CHAPTER III	EXPERIMENTAL METHODS	21
	Evaporation Mask Fabrication	23
	Heater Stage and Temperature Controlling System	26
	Evaporation Sources	27
	Sample Preparation	29
	Alloying	33
CHAPTER IV	EXPERIMENTAL RESULTS	35
	Early Problems With The Au-Sb Alloy	35
	Testing and Evaluation of Completed Devices	36
	Measurement of the Diode Photovoltage	40
CHAPTER V	SUGGESTIONS FOR CONTINUED RESEARCH AND CONCLUSION	42
	Etching and Polishing	42
	Heat Sinking	42
	Bonding	43
	Lifetime Measurements	45
	Conclusion	45
REFERENCES		46

LIST OF ILLUSTRATIONS

	Page
Fig. 1 -- Structural Arrangement of a p-i-n Photovoltaic Cell	7
Fig. 2 -- Proposed Planar TPV Cell Geometry	10
Fig. 3 -- Illustrating the Effect of Series Resistance on V-I Characteristics	11
Fig. 4 -- Absorption Coefficient of Germanium as a Function of Energy and Wavelength	14
Fig. 5 -- Hypothetical Paths of Holes and Electrons Generated on the Plane at $x = 0$	16
Fig. 6 -- Conduction Analogs for Series-Resistance Evaluation	19
Fig. 7 -- Evaporation Jig and Mask With 1 cm^2 Germanium Sample	24
Fig. 8 -- Jig for Machining Evaporation Mask	25
Fig. 9 -- Al Prepared for Evaporation	28
Fig. 10 - Au-Sb Prepared for Evaporation	30
Fig. 11 - Polishing Jig	32
Fig. 12 - Backside of Completed Diode	34
Fig. 13 - Au-Sb Alloyed Fingers Showing Segregation of Gold	34
Fig. 14a V-I Characteristic of Diode D3 Before Etching	38
Fig. 14b V-I Characteristic of Diode D3 After Etching	38
Fig. 15 - Longitudinal Cross Section of n+ Finger Showing Construction and Stitch Bonds	44

CHAPTER I

INTRODUCTION

The concept of a thermophotovoltaic energy converter was first proposed by Aigrain[1]; it emerged from considerations of thermoelectric converters in which the high temperatures needed for efficient conversion placed conflicting requirements on the electronic properties of materials and their thermal-physical properties. The excitation of electrons by radiant energy in a solid has the advantage that in some solids this ambipolar generation of electron-hole pairs is relatively weakly coupled to the lattice, having relaxation times of the order of 10^{-6} to 10^{-3} seconds.[2] It is, therefore, possible to produce large disturbances in electron distribution while the lattice is kept cool as a consequence of the limited rate of energy transfer from the electronic system to the phonon system.

In the field on photovoltaic converters the concept of a two step thermal-to-radiant-energy and radiant-to-electrical-energy conversion process is of interest because such a converter has more degrees of freedom than conventional solar cell systems. The source spectrum may be controlled to match the energy gap of the converter material, which allows the possibility of using materials other than silicon for photovoltaic devices. The future development of high intensity, controlled spectrum sources will allow the realization of portable electrical energy sources with a watts/pound ratio greater than any source presently available.

Germanium has been chosen as the device material for most investigations of thermophotovoltaic converters for several reasons. In germanium the wavelength of light which

will result in efficient energy conversion lies in the range of 1.5 to 1.6 microns.[3] According to Wien's Displacement Law, this corresponds to the peak radiation from a black body in the range of 1810°K to 1930°K. A source operating in such a temperature range is not difficult to acheive. Since germanium has been in use as a device material for so long, its technology has been perfected to a larger degree than any other semiconductor. Compared with silicon, germanium is available in higher degrees of physical perfection, with longer minority carrier lifetimes, and lower carrier trap densities. It is, therefore, a potentially more efficient photovoltaic conversion material than silicon.

Previous work on the thermophotovoltaic energy converter has been concerned primarily with the device geometry shown in Fig. 1. This configuration suffers from many ills which have manifested themselves in poor experimental results. Carriers are generated in the low lifetime n+ region, which tends to reduce the collection efficiency because of the considerable recombination which occurs in this region. Series contact resistance modifies the shape of the theoretical V-I curve of the device, reducing the maximum output power and saturating the efficiency. Ohmic contacts to the n+ front surface are difficult to obtain, and if they are designed to reduce series resistance effects, they mask a portion of the front surface from the incident radiation and make antireflection coating difficult. Perhaps the greatest drawback of this geometry is inherent in the fabrication technique. The device must be temperature cycled on three separate occasions during its construction: to 600°C for the n+ diffusion, to 550°C for the p+ alloy, and to 230°C for the evaporated front surface contacts. It has been pointed out by R.J. Schwartz and C.W. Kim[4] that

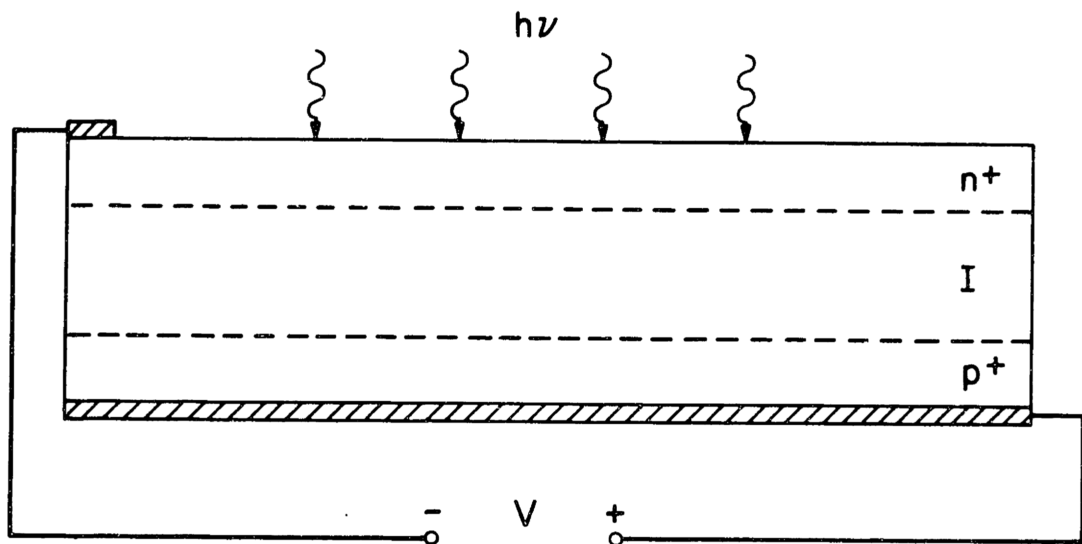

(a) One-Dimensional TPV Device

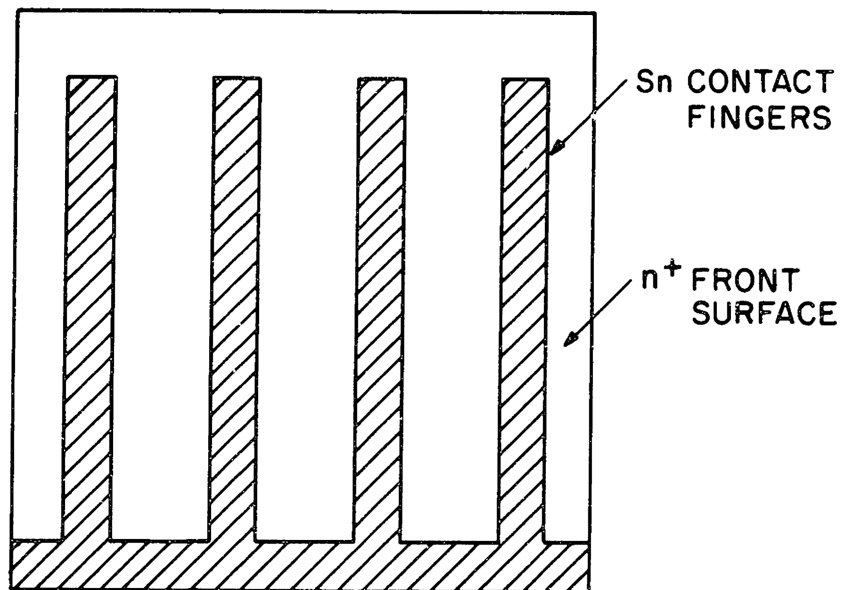

(b) Front Surface Contacts Designed to Reduce Series Resistance of One-Dimensional TPV Device

Fig. 1 Structural Arrangement of a p-i-n Photovoltaic Cell

cycling intrinsic germanium to temperatures in excess of 500°C seriously impairs the lifetime of the material. Lifetime measurements performed by Hewes[5] on completed devices have confirmed the fact that the lifetime has been considerably reduced during the fabrication process. As a result, the open-circuit voltage saturated at 260 millivolts with an intensity of approximately 10 watts/cm^2, in sharp contrast to the expected 400 millivolts at this intensity. The reduction in lifetime is undoubtedly due to diffusion of contaminants, especially copper, during the heat cycles. Such contamination is the cause of thermal conversion of high resistivity n-type germanium to p-type during a heat-quench cycle.[6] It has also been observed that thermal conversion is accompanied by a sharp decrease in the lifetime of minority carriers in germanium.[7] The cure is extreme cleanliness during fabrication, a solution which becomes more difficult as the number of steps in which contaminant diffusion may occur is increased. The maximum efficiency reported by Hewes and Siegel for their devices is 1.30%.[5] This is well removed from the figures of 20% to 30% which are often quoted as theoretically attainable. (see references 5, 8, and 9).

CHAPTER II

THE PLANAR p-i-n THERMOPHOTOVOLTAIC CELL

The device geometry with which this thesis is concerned is pictured in Fig. 2. The construction is planar, with both the p-i and n-i junctions on the back side of the germanium substrate. These junctions are alloyed simultaneously and at a relatively low temperature so that bulk lifetime is preserved. The front surface through which the radiant energy enters the cell is free from obstructions due to contact fingers, and the process of preparing the surface to reduce reflections is simplified. Surface recombination is reduced because contamination due to the fabrication of finger contacts is avoided. Of great importance is the fact that photon absorption and carrier generation now take place in the high lifetime intrinsic region. The large number of fingers and extensive contacting area reduce considerably the series resistance effects of the n+ diffused layer in the device shown in Fig. 1*.

Table I lists the factors affecting conversion efficiency and summarizes the comparison between the two geometries. Numbers for the one-dimensional device are those calculated by

---

* The effect of series resistance in the one-dimensional structure is shown in Fig. 3.[10] Although the open circuit voltage is not affected, the decrease in maximum power obtainable from the device is evident. In his preliminary experimental investigations, Siegel[10] has shown that the V-I characteristic for the planar device has the same form as that for the one-dimensional p-i-n structure. It is reasonable to assume, therfore, that series resistance will have the same qualitative effect on the planar device as it does on the one-dimensional device.

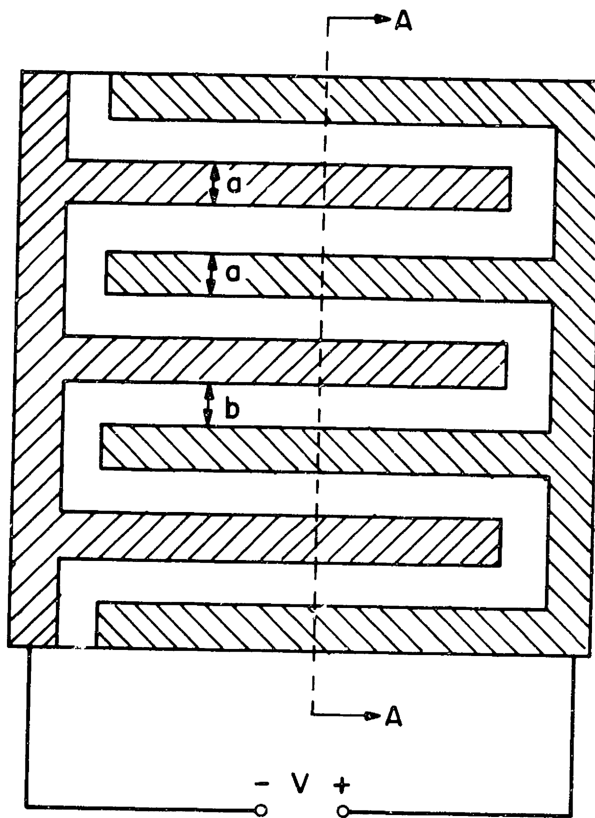

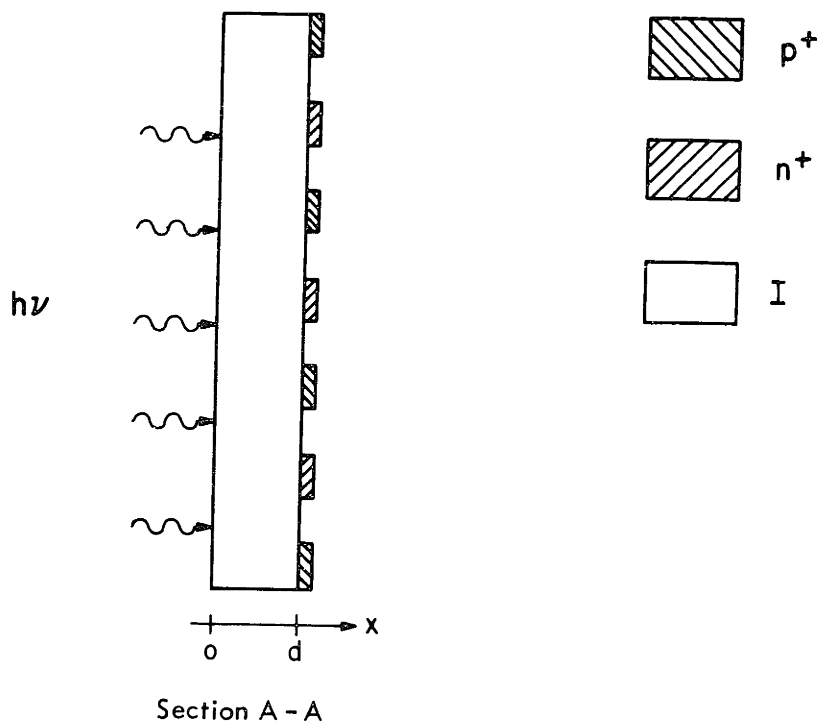

Fig. 2 Proposed Planar TPV Cell Geometry

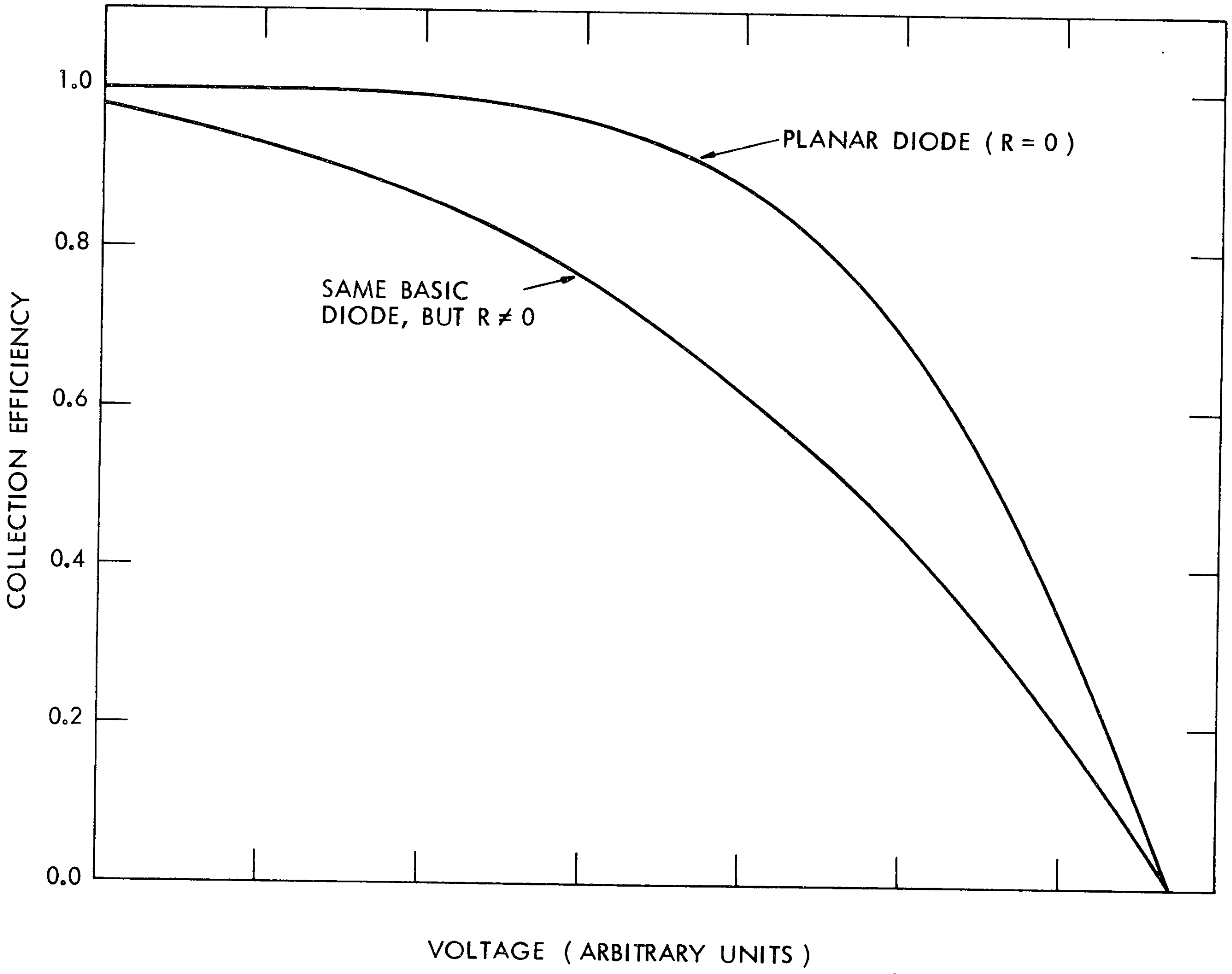

Fig. 3 Illustrating the effect of Series Resistance on V-I Characteristics

Siegel.[10] Numbers for the Planar device have been estimated considering the effects of improved surface treatment and the absence of the low lifetime n+ diffused layer.

TABLE I

FACTORS WHICH INFLUENCE CONVERSION EFFICIENCY

Parameter	One dimensional device	Planar device
Surface recombination	limits collection efficiency, Q_{sc}, to 38%	Q_{sc} = 75%
Reflection loss	64% transmission (no antireflection coating)	T = 64%
Source efficiency	27% of incident photons have E > 0.68 volts	27%
Collection efficiency at I_{max} power.	0.7 Q_{sc}	0.9 Q_{sc} due to reduction of series resistance
Voltage at maximum power	350 mv (10 w/cm^2)	350 mv
Theoretical efficiency	2.01%	5.10%
Actual efficiency of constructed device	1.30%	?

If source efficiency is improved and reflection losses eliminated, the planar device may easily reach an efficiency of 20%. Operating at higher injection levels will increase the open-circuit voltage of the planar device because of the increased bulk lifetime and will improve efficiency even further.

The research described in this thesis has been carried through the fabrication of the planar diode. Time and facilities did not permit the mounting, bonding, and detailed testing

of the completed TPV device. Suggestions for continued research along these lines have been included and should prove useful to those endeavoring to bring the TPV convertor to fruition.

Optimum Parameters For a Planar Device

Reference to Fig. 2 shows that there are three parameters of the planar device which must be determined; the finger width, a; the finger spacing, b; and the device thickness, d. These parameters must be optimized with respect to collection efficiency and series resistance.

a) The Variation of Collection Efficiency With d   It has been shown by Wedlock[3] that for the one-dimensional device the optimum thickness of the i-region lies between an absorption length and a diffusion length. Since the arguments used by Wedlock in his derivation are applicable to the two-dimensional case, d should also lie between an absorption length and a diffusion length. The diffusion length in intrinsic germanium is on the order of 0.25 mm.[11] The absorption length varies quite rapidly near the band edge of germanium (Fig. 4) but since we are only interested in radiation lying above E_g, a value of 0.10 mm has been taken for the maximum intrinsic absorption length. For optimum collection efficiency, therefore, d should lie between 0.10 mm and 0.25 mm.

b) The Variation of Collection Efficiency With a and b
It is immediately apparent that to prevent those carriers that reach the plane at x = d from recombining on the germanium surface between the alloy fingers, b must be zero. Of course this is impossible but it is clear that b should be made as small as possible.

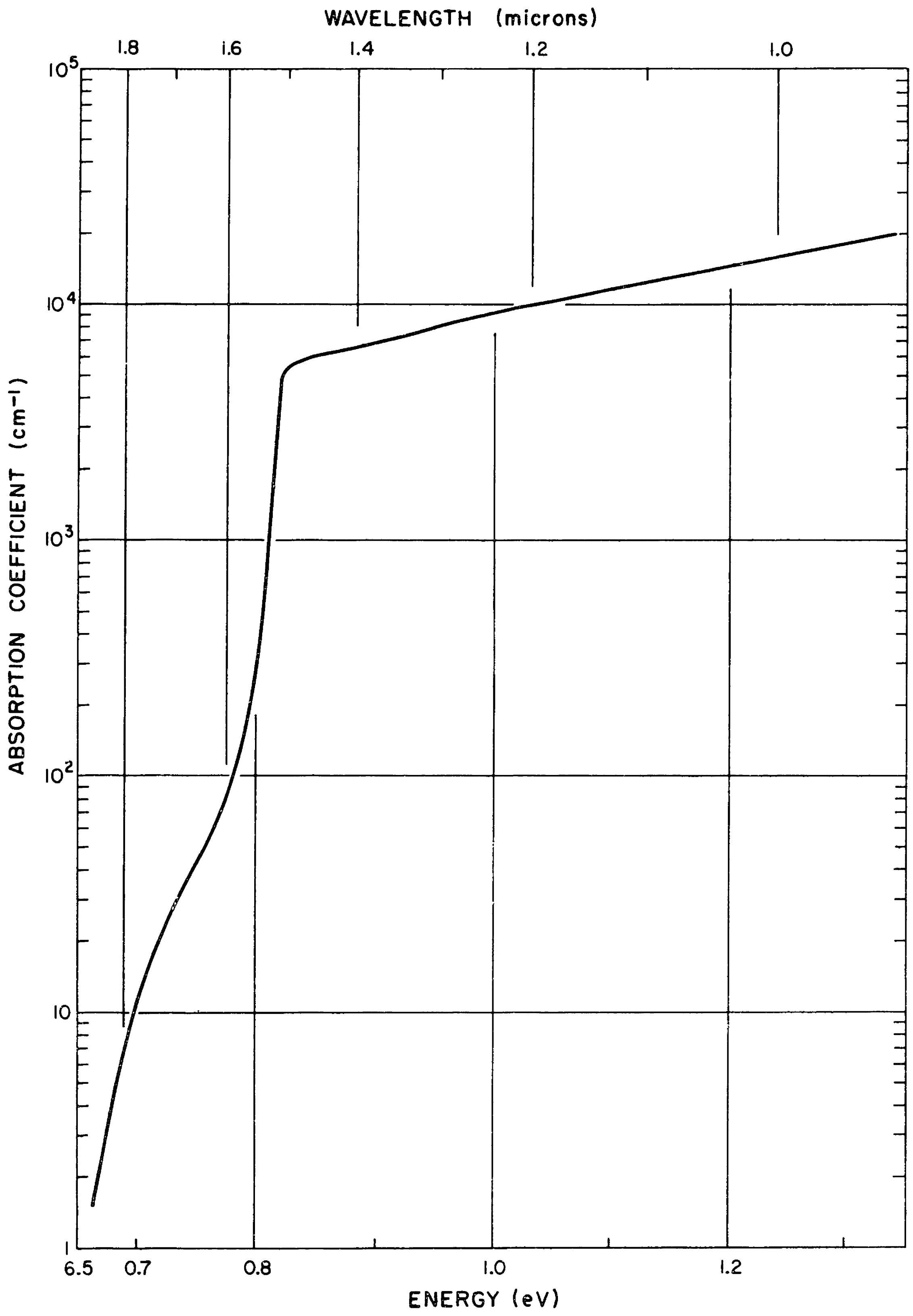

Fig. 4 Absorption Coefficient of Germanium as a Function of Energy and Wavelength

A flow pattern for hole-electron pairs generated near the front surface at x = 0 is shown in Fig. 5. Although the paths shown are not precise, it is true that holes must be collected at the i-p+ junction and electrons at the i-n+ junction and that the paths of these carriers can be no shorter than the straight lines shown in Fig. 5. Since from structural consideration d cannot be much less than a diffusion length, the paths in Fig. 5 should be as nearly perpendicular to the planes at x = 0 and x = d as possible. This leads one to conclude that for optimum collection efficiency both a and b should be as small as practicable, i.e., the number of fingers should be maximized.

c) The Variation of Series Resistance With a, b, and d

The calculation of series resistance for the planar device, as a function of the parameters a, b, and d and the conductivity profile under high level injection conditions, is a difficult task involving the solution of Laplace's equation for periodic boundary conditions on a finite surface. Although the problem is not impossible to solve mathematically, its solution was not considered to be of enough importance to justify such a significant expenditure of time and effort. Instead, a two-dimensional conduction analog was constructed of Teledeltos paper* and the result of measurements on this analog were extended to the third dimension.[12] Although this method does not take into account either the non-uniform conductivity under injection conditions, or the fact that the current flow in the device is not really two-dimensional due to the finiteness of

---

* Electrically conductive paper, available from: Development and Research Dept., The Western Union Telegraph Co., 60 Hudson Street, New York 13, New York

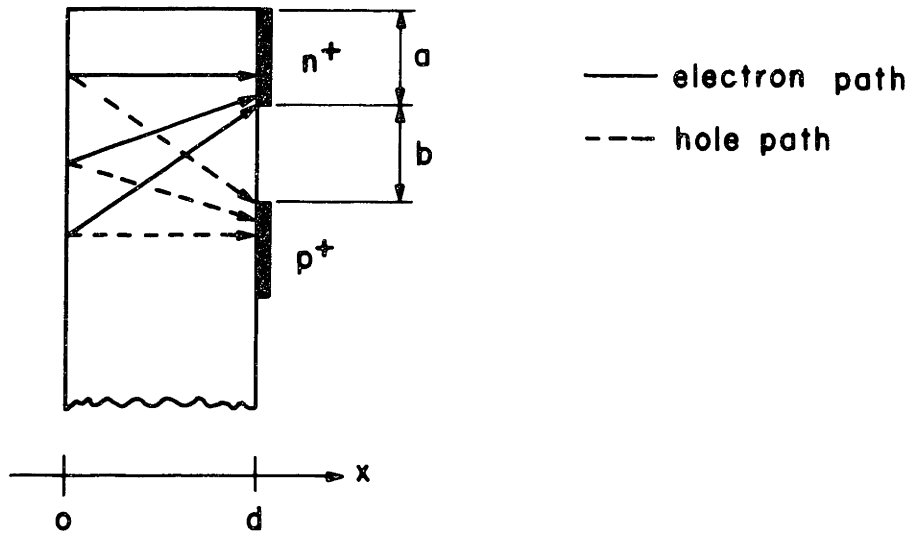

Fig. 5 Hypothetical Paths of Holes and Electrons Generated on the Plane at $x=0$

the third dimension, the analog does provide insight to the nature of the series resistance, its approximate behavior with variations of a, b, and d, and a numerical value for the series resistance under conditions of small injection.

Analog Evaluation of Series Resistance

Teledeltos paper was originally developed for use with strip chart recorders employing an electric pen. The paper has a very thin electrically-conducting coating on its surface. Potentials applied to various points on the surface produce current flow. Because the thickness of the layer is in general much smaller than its other two dimensions, the current density in the layer is essentially independent of the coordinate normal to the paper at any but the smallest distance from the electrodes and the current flow is two dimensional. Conduction in the layer can thus be used to obtain plots for two-dimensional electrostatic and magnetostatic fields in source-free regions. Boundary conditions are applied with either conducting paint or a pair of scissors. A cut in the paper forces the electric field to be tangential to the contour of the cut. Silver paint applied to the Teledeltos paper increases the conductivity in the painted region sufficiently so that the surface current density emerges normal to the contour of the painted areas (i.e., the painted area is an equipotential).

In the device geometry under consideration, the current flow is two-dimensional everywhere except at the boundaries. Since we are not actually interested in the flow pattern, but rather the total resistance between the two sets of fingers, the third dimension must be used in transforming from the measured sheet resistance of the Teledeltos paper analog to the bulk resistance of the device. The resistance of the device

is related to the measured resistance of the analog by

$$R = \frac{1}{\sigma t} \times \frac{R_1}{\rho} \qquad (1)$$

where R_1 is the measured resistance of the analog, σ is the conductivity of the device material, ρ is the ohms-per-square surface resistivity of the Teledeltos paper, t is the depth of the device in the third dimension, and R is the total bulk resistance of the device. This formula simply states that the actual resistance is the measured resistance weighted by the ratio of the sheet resistivities of the Teledeltos paper and germanium. The "sheet" resistivity of the germanium, $1/\sigma t$, is for a sheet of width t, i.e., "edge-on" for the device.

Two analogs with different values of a and b were constructed as shown in Fig. 6. A dimensional scale of 100:1 was used. The paper was cut to the proper size and mounted on a strip of masonite. Boundary conditions were applied with silver paint, keeping the dimension analogous to the diffusion depth as shallow as possible. The silver strips were appropriately connected with two strings of copper test clips. Calculations were made for a 1 cm^2 device. The device with the narrower fingers yielded a series resistance of 3.20 ohms while the device with three times the finger width exhibited a series resistance of 5.90 ohms. The resistivity of the germanium was taken to be 40 ohm-cm. On the basis of these results, and with the limitations of this analog technique in mind, it seems reasonable to assume that the series resistance of the device will be minimized if the density of fingers is maximized for a given spacing. This conclusion coincides with what one feels intuitively, that for a given voltage, the number of current paths and hence the conductivity, is proportional to the

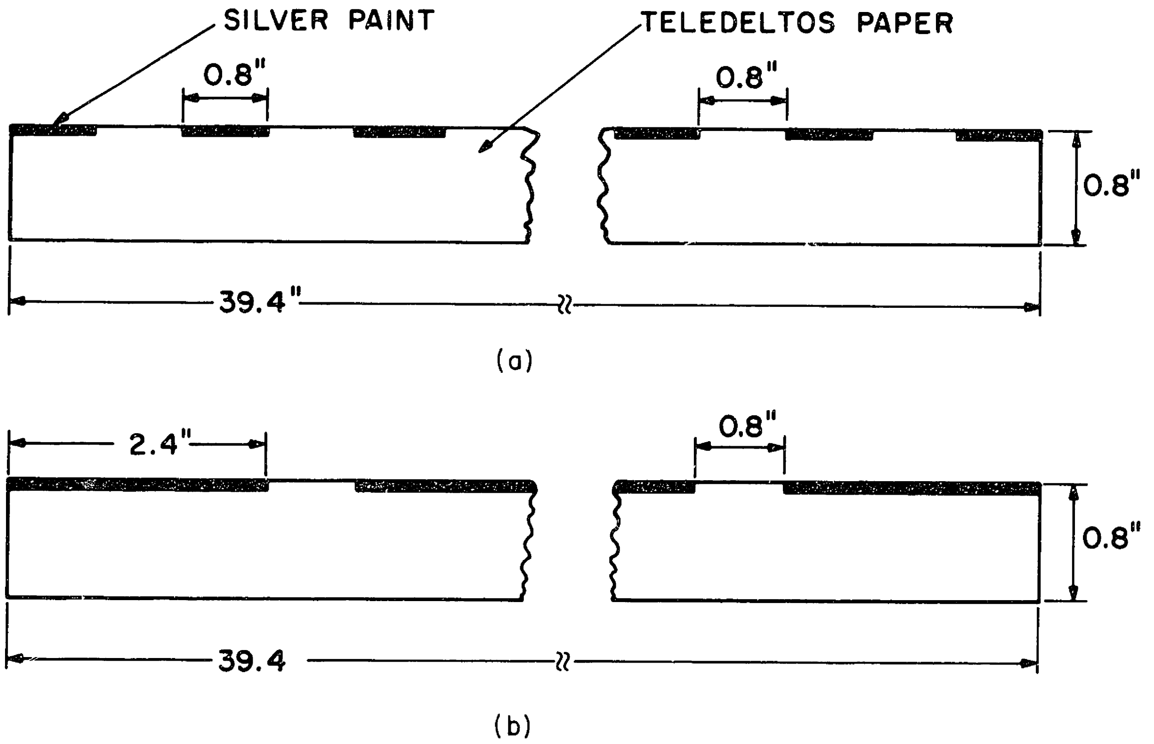

Fig. 6 Conduction Analogs for Series Resistance Determination

density of the fingers. This result is compatible with the conditions that influence $\underline{a}$, $\underline{b}$, and $\underline{d}$ with respect to collection efficiency.

The result of the investigation of collection efficiency and series resistance variations with geometrical device parameters is that the thickness, $\underline{d}$, of the device should be between a diffusion length and an absorption length, and the fingers should be as narrow as possible and as close together as practically attainable.

CHAPTER III

EXPERIMENTAL METHODS

The first decision which had to be made in the fabrication of this planar device was whether to use alloy or diffusion techniques in forming the n+ and p+ regions of the diode. The diffusion technique has the advantage of greater resolution of the finger structure but at the same time it presents major fabrication difficulties. Paramount amoung these difficulties is the inability to form easily, a protective mask on the germanium such as the oxide used in the fabrication of diffused silicon devices. The high temperatures required during diffusions will invariably reduce the bulk lifetime of the material. Without much difficulty, alloyed fingers may be made 0.008 inches wide. Considering the results of the Teledeltos analog, the series resistance of the 0.008" geometry is 3.2 ohms. This is the resistance of the unilluminated diode. Under high level injection conditions conductivity modulation will reduce this resistance by several orders of magnitude, making the 0.008" finger dimension acceptable. With the proper choice of metals, both fingers may be alloyed at the same time and at a relatively low temperature. It was decided, therefore, to form the n+ and p+ regions of the device by alloying. Vapor deposition of the metal was chosen instead of foil strips because the narrowness of the fingers would present handling problems if foil were used.

Aluminum was chosen as the alloying metal for the p+ fingers. It is easily evaporated from a tungsten filament, adheres well to germanium, and forms a relatively low temperature (424°C) eutectic with germanium. Aluminum readily accepts

a gold wire thermocompression bond so that if it is deposited in sufficient quantity initially, no further contacting metal need be applied to the p+ fingers.

Arsenic and antimony are the metals generally used for n-type alloy junction formation. Both are hard, brittle metals with low vapor pressures and require special precautions in their use. Both metals require a carrier to speed up the diffusion process at reasonable temperatures. Lead or gold is generally used because of the low Au-Sb or Pb-Sb eutectic. The use of such a soft metal also makes the resulting eutectic maleable thereby preventing the cracking which would occur on cooling if antimony or arsenic were used alone. The solubility of arsenic in germanium is larger than that of antimony by about an order of magnitude.[13] The toxic nature of arsenic, however, requires that it be evaporated in a closed system. A mixture of gold and antimony was chosen and the possibility of adding a few percent As was kept in mind for future experimentation. Such a mixture has been used with good results by Przybylski and Roberts in the fabrication of tunnel diodes.[14]

Considering the results of the investigation described in the previous section of this report, the following dimensions for the device were decided upon:

$$a = 0.008''$$
$$b = 0.008''$$
$$c = 0.008''$$

The minimum finger width and spacing were dictated by two considerations:

1) jeweler's saw blades cannot be obtained in thicknesses less than 0.006". This blade produces an 0.008" slot in the evaporation mask.

2) the finger must be wide enough to accept a stitch bond.

Evaporation Mask Fabrication

Due to the close tolerances imposed by the interdigitation of the evaporated metal fingers, the evaporation mask fabrication was a major concern. A total of 10 masks were machined using various techniques. Of these 10, only 2 were acceptable for use. The type of mask under discussion is illustrated in Fig. 7. The mask must have a reference edge for alignment in the jig to be described later, and all the slots must be parallel to this edge. The metal must be as thin as possible to prevent "shadowing" during the evaporation and yet thick enough to machine and lie flat. The length of the slots must be calculated carefully, taking into account the thickness of the metal and curvature of the blade at the cutting point on its circumference.

The stock from which the good masks were made was 0.012" mild cold rolled steel. A jig for holding this metal in the milling machine was made from a block of aluminum and not removed from the chuck of the miller until the masks for both sets of fingers were completed as shown in Fig. 8. Both masks were machined at the same time from the same piece of sheet steel. This constrained the measureing reference to be identical for both masks, i.e., the edge of the aluminum block.

The jeweler's saw blades with which the slots were cut is a very ill behaved tool. It has a tendency to clog, break teeth, and "walk" when a slot of unreasonable depth is being cut. To minimize the effect of curvature, the blade was lowered 0.180" beneath the surface of the work. This depth gives a well defined end to the slot. Slots were first cut in the

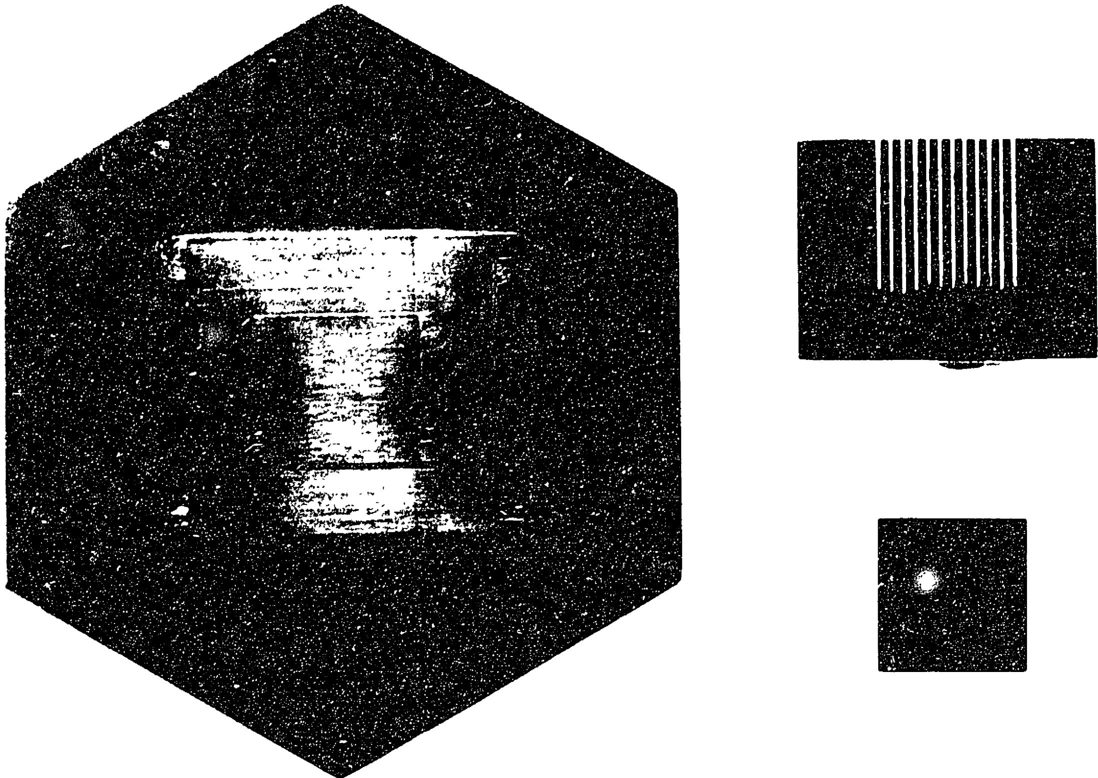

Fig. 7 Evaporation Jig and Mask with 1 cm^2 Germanium Sample

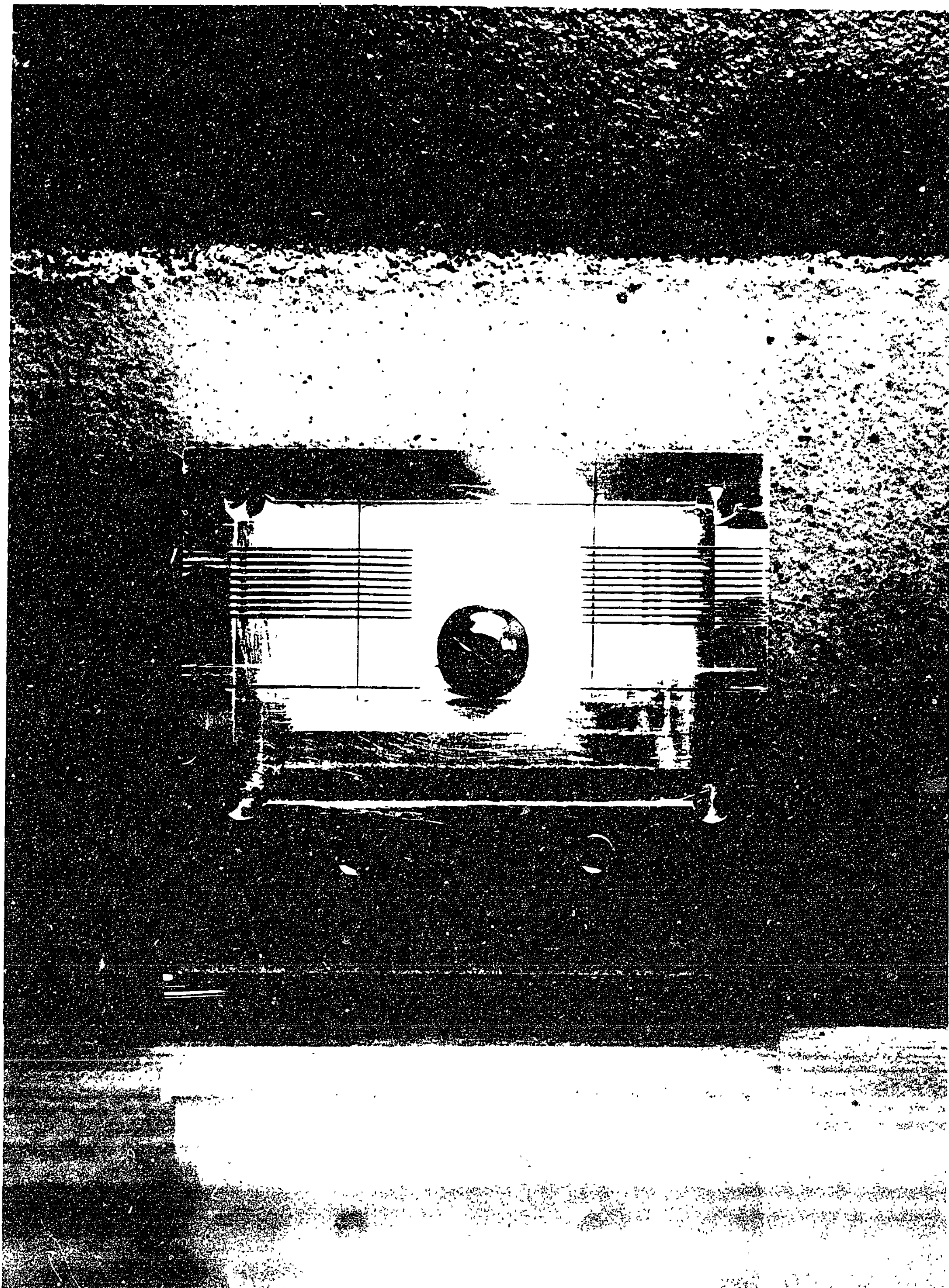

Fig. 8 Jig for Machining Evaporation Masks

Screw in center is for holding blank of cold rolled steel. The two holes in the foreground are for clamps which hold down edges of the blank.

aluminum jig with a 0.010" blade so that the more delicate 0.008" blade would have to cut only the steel. This precaution increased the life of the blade immeasurably and enabled both masks to be cut with the same blade, a definite advantage since each blade has slightly different physical characteristics. Whenever a blade was replaced, a test slot was cut to check the new blade for a tendency to "walk", i.e., not cut parallel to the reference edge of the jig.

After machining, the masks were carefully deburred, degreased, and polished. They were then measured under a metallurgical microscope to ascertain that the dimensions were within the specified tolerances.

A jig for holding and aligning the masks and sample in the evaporator was machined from stainless steel (see Fig. 7). Tolerances on the jig are 0.001" and consequently the masks can be changed with the guarantee that the fingers will "interlock" properly. Two concentric holes were drilled in the side of the jig to accept a thermocouple and its insulating alumina tube. The sensing junction of the couple was located directly beneath the sample depression in the jig.

Heater Stage and Temperature Controlling System

A simple heater for alloying within the evaporator was made by removing the thermostatic controls from a hotplate and mounting the plate with its internal heating coil on a stainless steel base. Leads were brought out the baseplate of the evaporator and connected to a variac. The stage was degassed for an extensive amount of time before being put into use.

The thermocouple used was of the chromel-alumel type. It was introduced into the evaporator through an octal plug without cutting the wires. This precaution was necessary to insure

that the reference junction was at the terminals of the potentiometer and not at the feedthrough inside the evaporator. The bare thermocouple wires inside the bell jar were insulated with alumina tubing. The tubing was broken at several places to make the system flexible. It was also shielded during all evaporations to prevent depositing metal from shorting the leads.

Manual control of the temperature was quite accurate and with a little practive both the final temperature and the rate of increase or decrease could be controlled within a degree.

Evaporation Sources

Fig. 9 shows the evaporator set up for the aluminum deposition. Approximately 400 mg of aluminum is loaded on a heavy tungsten coil filament. The aluminum in wire form is cut into four pieces and each piece looped over a turn of the coil. This prevents the molten aluminum from shorting adjacent turns of the filament, a result which occurs if the wire is simply folded and inserted into the coil. The filament must be quite heavy so that it is not completely dissolved by the large amount of molten aluminum. The source is placed almost directly over the substrate to minimize shadowing.

The gold-antimony deposition is a more complicated affair. Antimony does not wet tungsten and most attempts to evaporate both metals from the same tungsten filament have resulted in a molten ball of Au-Sb alloy dripping off the filament. Due to complications to be discussed later it was found necessary to deposit the antimony over the gold, the reverse of the sequence which occurs if both metals are evaporated from the same heater. Consequently, a seperate filament of chromel was wound for evaporating the antimony. Antimony wets chromel quite readily.

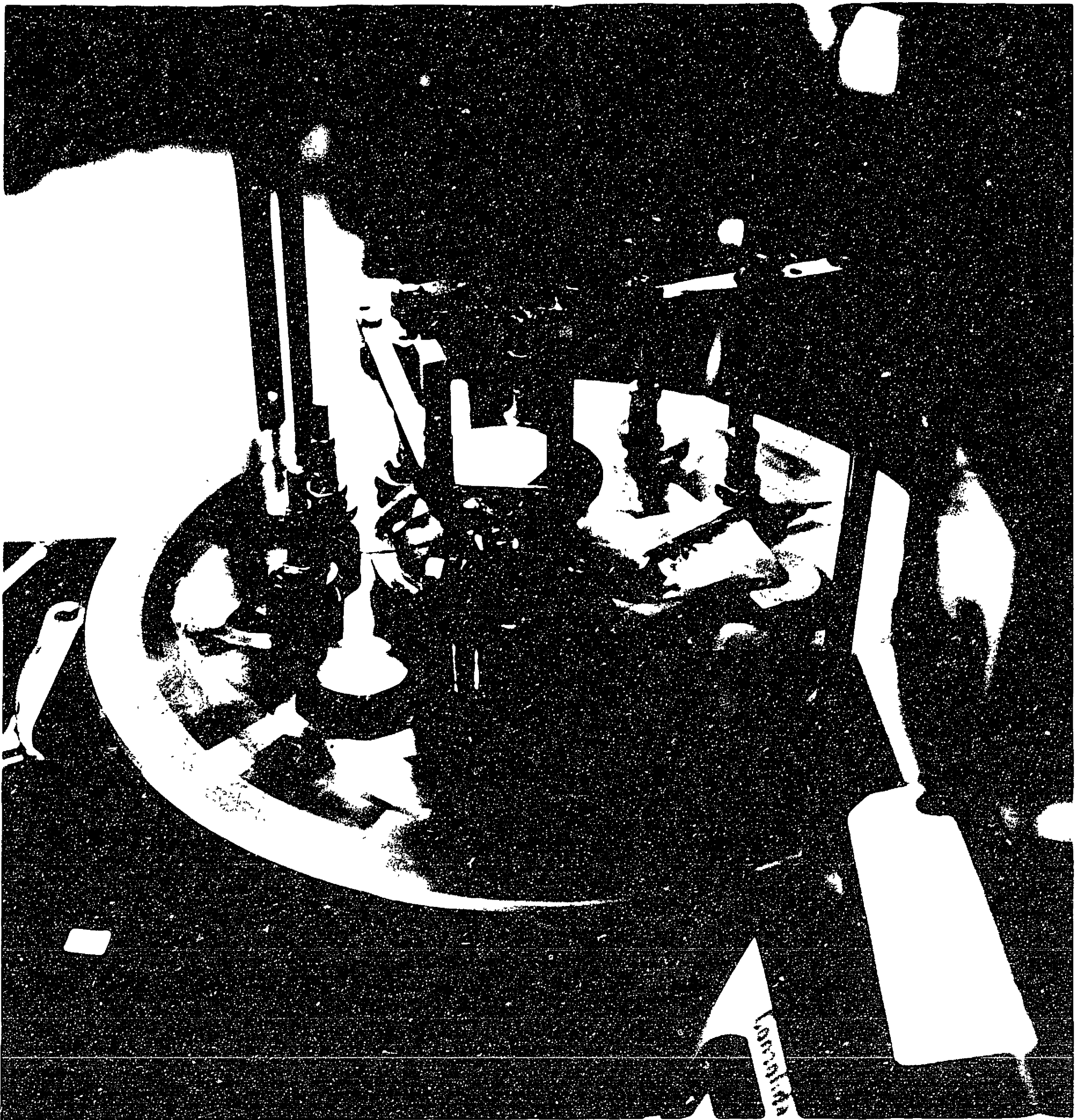

Fig. 9 Al Prepared for Evaporation
Feedthrough for Thermocouple is in Foreground

The low melting point of the metal, however, makes evaporation control, and especially degassing of the source, quite difficult. The evaporating temperature is approximately 675°C, just about the same temperature at which the filament is beginning to glow dull red. With the small amount of metal being used, one must take care not to evaporate it before desired.

The gold is evaporated from a conical tungsten filament and no problem has been encountered. Since the gold is evaporated first care must be taken to shield the Sb source so that the gold does not contaminate it and prevent its wetting the chromel filament as shown in Fig. 10.

Before all evaporations the substrate is brought up to about 150°C and degassed for 10 minutes. At the same time the sources are made to wet the filament and evaporate slightly. The shield over the sample is then removed and the metal deposited. Between the Al and the Au-Sb evaporations, the sample is allowed to cool, the vacuum is broken and the mask is changed.

Before being placed in the evaporator the sources and filaments are carefully cleaned. After being degreased in trichlorethylene they are rinsed in running methyl alcohol and washed ultrasonically in a solution of Igepol detergent for a period of 3 minutes. They are then vigorously rinsed in running distilled, demineralized water, then methyl alcohol followed by acetone followed by methyl alcohol again. Until being placed in the evaporator they are stored in a covered beaker of methyl alcohol. All sources are, of course, taken through these steps separately.

Sample Preparation

Square substrates, 1cm x 1cm x 0.04cm, are cut from a

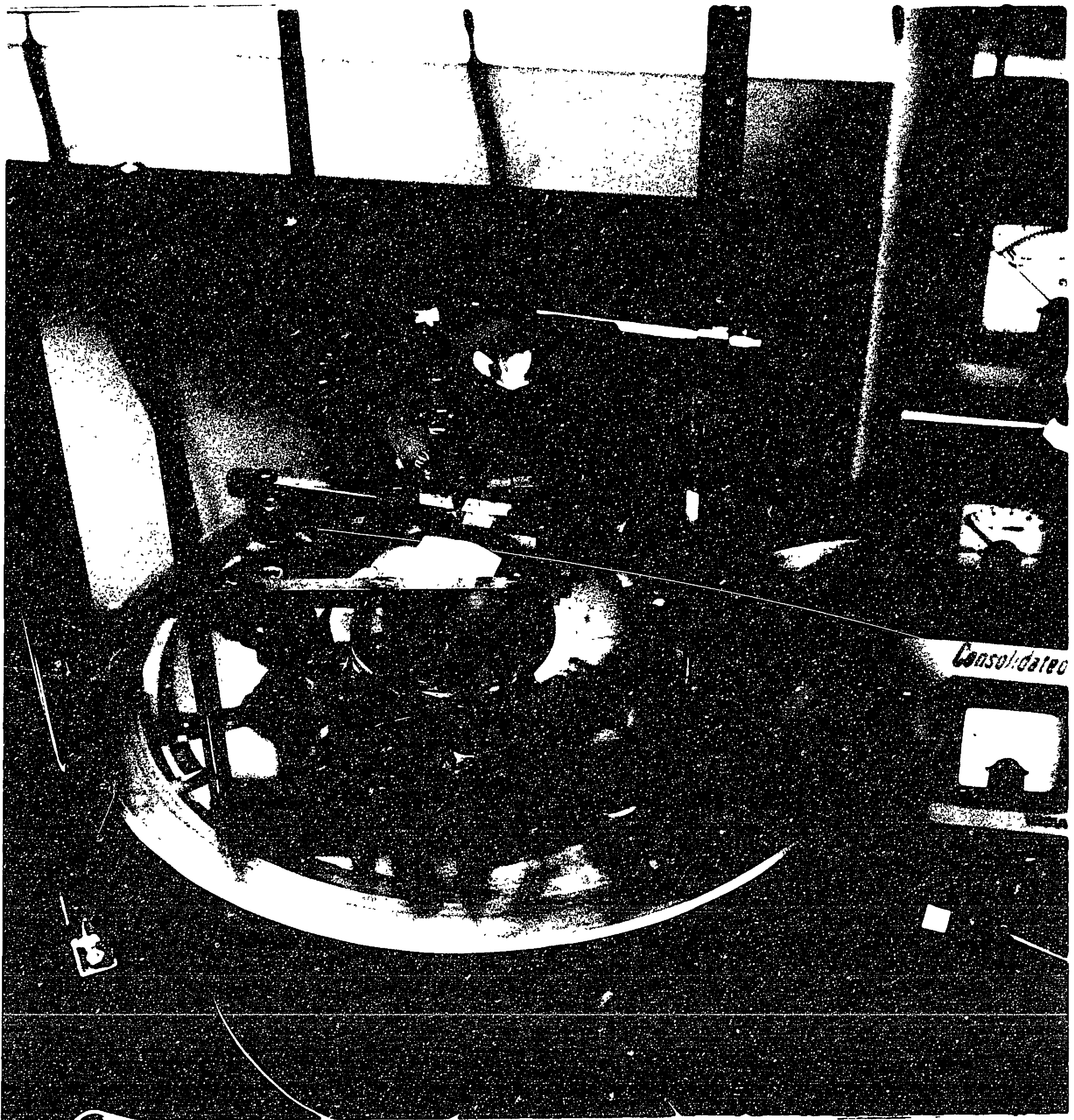

Fig. 10 Au-Sb Prepared for Evaporation

The chromel filament charged with antimony is to the right of the shield. The conical tungsten filament is to the left. In the center of the evaporator is the substrate heater for alloying. To the right of the heater is the alumina thermocouple tubing and the degassing shutter.

40 ohm-cm germanium crystal on a diamond saw. These substrates are then mounted with wax on a polishing jig (Fig. 11) and lapped to a thickness of about 0.010". "Wet or Dry" silicon carbide paper is used for the lapping, starting with 400 grit and finishing with 600 grit. Without removing the sample from the jig it is polished on a metallurgical wheel, first with 0.3 micron alumina powder (Linde "A") and finally with 0.05 micron alumina (Linde "B"). Extreme care must be excercised in cleaning the jig and germanium between the two final polishes to insure that no Linde "A" is transferred inadvertantly to the finish polish wheel. A gentle wash with Ivory soap applied with a cotton swab is generally sufficient for the sample but the ring of the jig is ultrasonically cleaned to remove the powder from the retaining screw and slot.

The polishing time until all visible surface damage disappears on the coarse wheel is noted and the polishing is continued on this wheel for again as long. It is a general rule of thumb that the invisible surface damage penetrates to a depth equal to the visible damage. Polishing is then continued on the "B" wheel for half the total time taken on the "A" wheel.

After being polished, the germanium sample is etched for 30 seconds in a solution consisting of one part hydroflouric acid, one part nitric acid, one part hydrogen peroxide (30%), and four parts of distilled, demineralized water. The etch leaves the surface with a mirror-like finish and a coarse grid of tiny, hairlike scratches. No amount of polishing has eliminated these scratches. A problem associated with them will be discussed later. After etching, the jig is heated and the sample carefully removed, washed in acetone, rinsed in methyl alcohol, blown dry, and stored in a covered petri dish.

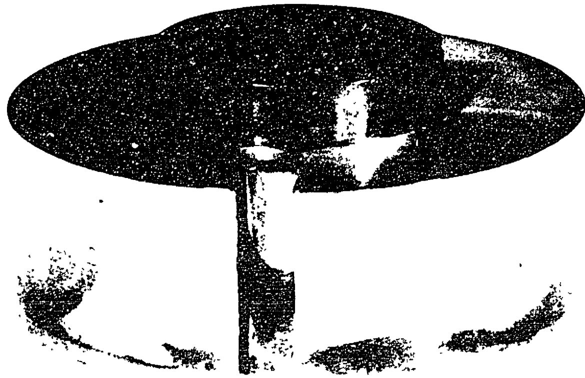

Fig.11 Polishing Jig

Alloying

Alloying of both the p and n-type fingers is done in a single step, without breaking the vacuum after the Au-Sb deposition. The jig and sample are heated to 425°C at a rate of from 3 to 5°/minute. The temperature is maintained at 425°C for 5 minutes and then it is lowered to 100°C at 3°/minute. At this point the vacuum is broken and a charge of gold is placed in the same filament used for the gold in the Au-Sb evaporation. The substrate is reheated to 150°C and this contact gold is deposited onto the n-type fingers through the mask which has not been disturbed since the Au-Sb deposition. The system is then cooled and the completed diode removed from the jig. Fig. 12 shows the backside of a completed diode.

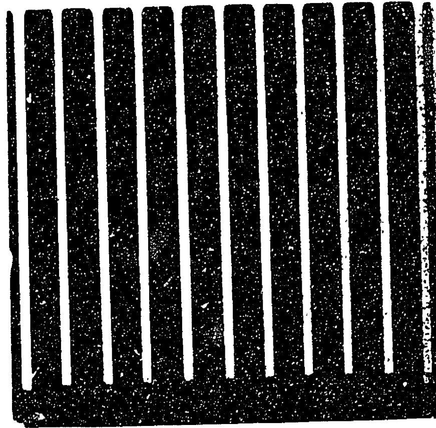

Fig. 12 Backside of Completed Diode (x6)

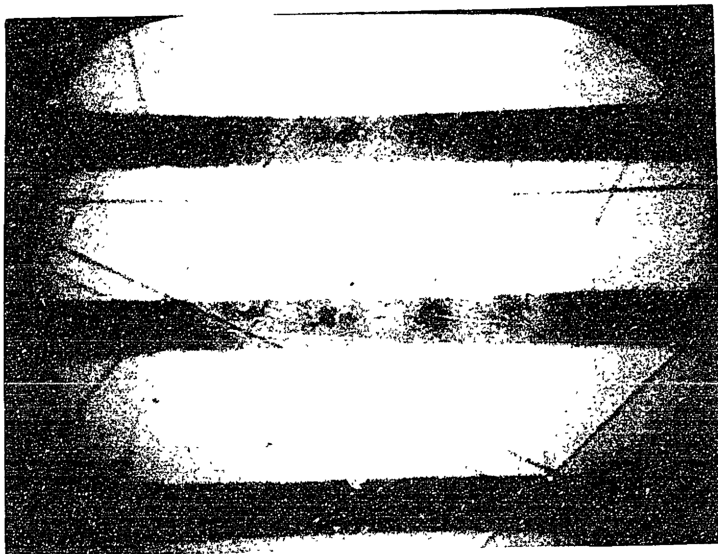

Fig. 13 Au-Sb Alloyed Fingers Showing Segration of Gold (x30)

CHAPTER IV

EXPERIMENTAL RESULTS

Early Problems With The Au-Sb Alloy

One of the major problems encountered during the course of this research was the tendency for the gold to ball on the n-type fingers during the alloying cycle. Fig. 13 illustrates this phenomenon; note that the finger is still well defined because of the antimony. Probe measurements indicated that n+-i junctions had formed in dissociated spots along the fingers, not necessarily at the gold balls. A mixture of 80% Au and 20% Sb was being used to fabricate these devices. The two metals were being evaporated from the same tungsten filament, the volume of antimony being sufficient to allow surface tension to hold the metal between adjacent turns of the filament as it was evaporating. As mentioned previously, this method of evaporation results in the Sb being deposited first.

Navon[15] has pointed out that if the amount of antimony in a gold-antimony alloying mixture exceeds 5%, the gold will not wet silicon. A series of alloying tests where only the n-type fingers were fabricated has shown that the same result holds for germanium. Gold with no antimony added was alloyed to the germanium with no evident tendency for the gold to ball. Additions of very small amounts of Sb, sufficient to form the n+ junction, did not induce balling. It was noticed, however, that the Au-Ge eutectic was of high resistivity and semiconductor-like. This observation necessitated the gold contact evaporation to reduce the series resistance and make ohmic contacts to the n-type fingers possible.

A further precaution taken to insure that the gold wets

uniformly is to deposit the gold before the antimony. Since the Au-Ge eutectic (356°C) is slightly below the Au-Sb eutectic (360°C) it was hoped that the gold would alloy with the Ge before it had a chance to ball due to the antimony. This procedure produced uniform wetting of the fingers.

It should be mentioned at this point that the evaporation of a small amount of antimony from a filament is not an easy matter. The chip of Sb must be large enough to be held in the filament coil until it melts and yet small enough so that it constitutes no more than 5% by weight of the deposited metal. The weight of the smallest practical chip was found to be about 20 mg, which required about 400 mg of gold to be evaporated, far more than necessary to form the junction. Evaporating only a small portion of the antimony source is a nice idea but somewhat impractical for the reasons stated earlier.

Testing and Evaluation of Completed Devices

Devices fresh out of the evaporator were first given a careful visual microscopic inspection to check for finger delineation, gold segregation, and mask alignment. The device was then placed on the stage of a probing machine and contact was made through two tungsten probes. The V-I characteristic of the diode was displayed on a Tektronix Model 575 transistor curve tracer.

Initially all devices tested exhibited the terminal characteristics of a resistor in the thousand ohm range, or a diode with an inordinately large and non-saturating reverse characteristic, i.e., a very leaky device. Careful microscopic inspection disclosed what looked like gold migration along the hairline scratches on the surface of the germanium. Dragging a probe across one of the scratches disjointed the fine gold

thread and lent credibility to the gold migration argument.

The removal of these leakage paths proved difficult as facilities for properly masking the fingers from an etch were lacking. After much trial and error it was found that a three second etch in aqua regia followed by a three second etch in concentrated HF removed a noticeable degree of the leakage but left the gold and aluminum fingers reasonably intact. As the gold is still visibly discernible in the scratches, it must be concluded that the etching process has merely dissociated the threads without totally removing them. Fig. 14a shows the V-I characteristic of diode D3 upon coming out of the evaporator. Fig. 14b shows the characteristics of the same diode after geing etched as described. The reverse characteristic is markedly improved. A more complete elimination of leakage paths could be effected by covering the fingers with positive photo resist exposed through the evaporation masks. The entire device could then be immersed in a superoxyl etch which would not only clean the germanium between the fingers but would etch some germanium from the edges of the device as well.

The forward characteristics of those devices tested displayed a significant amount of series resistance. From the results of the Teledeltos analog, one expects the internal series resistance of the device to be in the vicinity of 3 ohms under conditions of low level injection. At a terminal current of 0.1 ampere, this resistance results in a forward voltage drop of 0.3 volts. Figure 14b is in rather close agreement with this result. The series resistance effect, however, is not observed to diminish at increasing current densities, as one would predict if only the internal device resistance were involved. The resistance of the point contacts and the metal fingers themselves must be taken into account at high current

a

V-I Characteristics of Diode D3 Before Etch

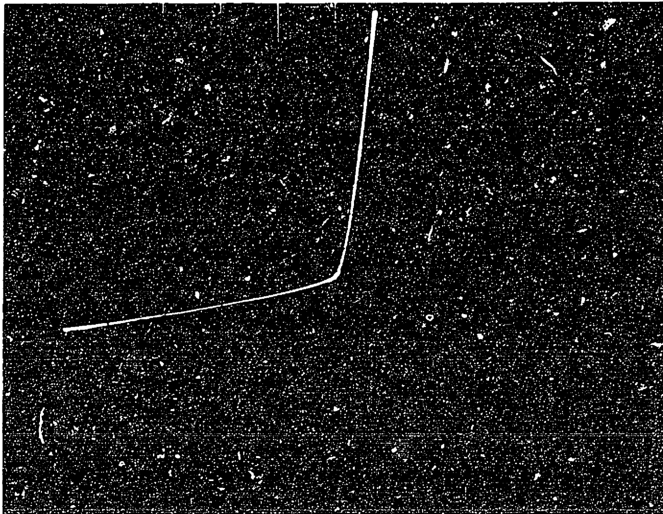

b

V-I Characteristics of Diode D3 After Being Etched for 3 Seconds in HF and 3 Seconds in Aqua Regia.

Fig. 14 Scale: Vertical = 50 ma/div.
Horizontal = 2 v/div.

levels when the device is being tested in the manner described. The behavior displayed by the forward characteristic in Fig. 14b is, therefore, not alarming and certainly predictable. In order to test the device more rigorously, it should be bonded in the fashion described later, which will eliminate the effects of contact resistance and series resistance of the fingers.

The saturation current of the diode may be estimated, rather roughly, by considering the dimensions of the device. Denoting the junction area by A, the minority carrier diffusion coefficient by D, the junction depth by W, the electronic charge by q, and the equilibrium minority carrier concentration in either the n+ or p+ regions by n, one obtains for the saturation current, I_s, of a p-i-n diode with very narrow i region:

$$I_s = \frac{nqAD}{W}$$

As the i-region is made wider so that recombination occurs within it, I_s will increase. The above formula, therefore, provides a lower limit on the expected value of the diode saturation current. For the device under consideration:

$$A = 0.20 \text{ cm}^2$$

$$D \cong 60 \text{ cm}^2/\text{sec}$$

$$n = 10^9/\text{cm}^3$$

$$W \cong 10^{-6} \text{ cm}$$

The value for n was based on the solid solubility of antimony in germanium, $10^{18}/\text{cm}^3$. The value of W is an educated guess based on the relatively short alloying time and low alloying temperature. Substituting these numbers into the equation for I_s results in a theoretical saturation current of 2 ma.

Reference to Fig. 14b shows that the actual saturation current is a little more than an order of magnitude greater than expected. Even after etching, the "saturation" current does not saturate which indicates that leakage paths still exist. A more exact determination of W is necessary before any further conclusions can be drawn about the nature and relative magnitude of the measured saturation current.

Measurement of the Diode Photovoltage

The open circuit voltage of diodes D3 and D4 were measured illuminating the diode from the back surface. The illumination source consisted of a microscope light focused on the exposed surface of the diode as it was held on the stage of the probing machine. Both diodes produced an open circuit voltage of approximately 60 mv. Although this is somewhat lower than the 100 or 200 mv expected to be produced by illumination from such a source*, one must bear in mind that the illumination is incident on the back surface, approximately half of which is covered by the finger structure. Carriers are generated only between the fingers resulting in a non-uniform distribution of carriers beneath the fingers. The back surface recombination velocity is undoubtedly quite large due to deposits of foreign matter and dissociated aluminum left by the etching process. Considering these factors the measured open circuit voltage is quite encourageing.

It was observed that under illumination the low current region of the forward characteristic of the diode shifted

---

* Siegel has privately reported an open circuit voltage of 200 mv produced by a microscope light focused on one of his two dimensional diodes.

slightly towards the V = 0 axis. If one argues that this shift is due to conductivity modulation, the previous discussion of the forward characteristic of the device is given further substantiation.

CHAPTER V

SUGGESTIONS FOR CONTINUED RESEARCH AND CONCLUSION

The following is an outline of problems in the fabrication of a planar thermophotovoltaic convertor still remaining to be solved, and suggested solutions or methods of attack.

Etching and Polishing

The use of positive photoresist to protect the fingers during the etch to eliminate leakage has already been discussed. The front surface of the device still remains to be polished. This should be done after the clean up etch. About 0.0005" of wax generally exists between the substrate and polishing jig when the sample is mounted carefully. This amount of wax is sufficient to protect the finger structure on the back side of the device if it is mounted back side down. The front surface is then polished using the same procedure that was used for the back surface in preparation for the metal deposition. At this stage it is a good idea to remove the germanium from the polishing jig not by melting the wax but by dissolving the wax in acetone, a process which generally takes a day. This precaution avoids any damage to the finger structure which might occur if the substrate were to slide on the melted wax as it was being lifted off the jig.

Heat Sinking

A major problem is anticipated in the removal of heat from the device during testing. Seigel[10] found that at an incident intensity of 10 w/cm^2. their devices required a considerable amount of cooling. Kim and Schwartz[4], who are working with the

planar geometry, found heat sinking to be one of their major problems even when using pulse techniques. Taylor[16] used a heat sinking compound to fasten his device to a water cooled brass plug. His fingers, however, were foil and the backside of the device was devoid of stitching. Considering all possibilities evident at this time, it is proposed that the device be mounted on a blank of synthetic sapphire and that the back side of the device be thermally connected to a water cooled brass plug with a bridge of heat sinking compound. Synthetic sapphire has the properties of good thermal conduction, 85% transmissivity at 1.1 microns, and machineability.[17] A series of holes may be drilled around the perimeter of the sapphire and cooling water passed through them. At the same time, a stream of cooled air may be directed at the face of the sapphire. The device will be cooled, therefore, from both its front and back surfaces. Even with such an elaborate scheme, it is not clear at this stage whether the cooling will be sufficient.

Bonding

The method of bonding necessary to eliminate the series resistance of the fingers is illustrated in Fig. 15 for one finger. Contact is made to the device by "stiching" down each finger with 0.001" gold wire using a thermocompression wire bonder. The stitch bonds will terminate on binding posts epoxied to the back side of the sapphire heat sink. Since optical cement generally breaks down at temperatures in excess of 100°C, the device must be bonded before being cemented to the sapphire substrate. For stitching purposes the diode may be held on an aluminum vacuum stage designed so that it may be mounted on the existing heat column of the bonding machine.

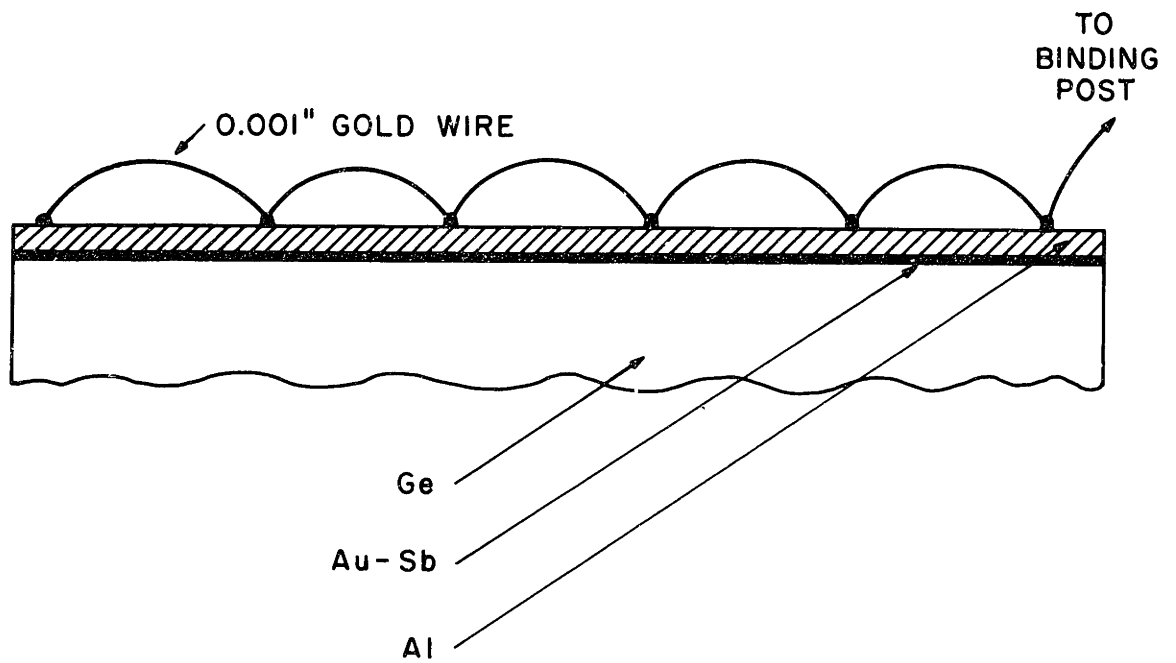

Fig. 15 Longitudinal Cross Section of n^+ Finger Showing Construction and Stitch Bonds

Lifetime Measurements

Since the arguments in favor of using the alloy technique for forming the n+ and p+ regions of the diode invoked lifetime preservation, some effort should be made to measure the lifetime of completed devices. Hewes[5] gives a detailed description of a method for determining the lifetime at high injection levels.

If lifetime deterioration is evident during the alloying process, both the masks and the jig may be machined from high purity molybdenum.

Conclusion

The developmental research done on the planar thermophotovoltaic energy converter has produced some very encourageing results. It has been demonstrated that a finger contact and junction structure fine enough to eliminate the effects of series bulk resistance at high injection levels is obtainable using evaporation techniques. A procedure has been developed for alloying both junctions at the same time without removing the device from the vacuum system. Hence handling and the possibility of contamination has been reduced and production equipment has been simplified.

Completed diodes show good characteristics and exhibit an open circuit voltage of 60 mv. Leakage paths have been isolated and the possibility of their removal demonstrated.

Further developmental work is required before the relative merits of the planar structure over the two-dimensional structure can be evaluated. Mounting and bonding remains the chief concern for future work. Suggested methods for bringing the device to completion have been outlined in this thesis.

REFERENCES

1. Aigrain, P., "The Thermophotovoltaic Converter", unpublished lectures given at MIT, Fall 1960 and Spring 1961.

2. White, D.C., Wedlock, B.D., and Blair, J., "Recent Advance in Thermal Energy Conversion", Proceedings, 15th Annual Power Sources Conference, May 1961.

3. Wedlock, B.D., "Spectral Response and Conversion Efficiency of P-N Junctions", Sc.D. Thesis, Dept. of Electrical Engineering, MIT, September 1962.

4. Schwartz, R.J. and Kim, C.W., Purdue University, private communication.

5. Hewes, C.R., "A Germanium Device For Thermophotovoltaic Energy Conversion", M.S. Thesis, Dept. of Electrical Engineering, MIT, October 1966.

6. Boltaks, B.I., Diffusion in Semiconductors, Academic Press, New York, 1963, p.167.

7. Burton, J.A., Hill, G.W., Morin, F.J., and Severiens, J.C., "Effect of Nickel and Copper Impurities on the Recombination of Holes and Electrons in Germanium", J. Phys. Chem., 853 (1953).

8. Wedlock, B.D., "Thermophotovoltaic Energy Conversion", Proc. IEEE, Vol. 51, pp.694, May 1963.

9. White, D.C., and Schwartz, R.J., "P-I-N Structures for Controlled Spectrum Photovoltaic Converters", Proc. 6th AGARD Conference, March 1964.

10. Siegel, R., "A Germanium Thermophotovoltaic Energy Converter", M.S. Thesis, Dept. of Electrical Engineering, MIT, September 1966.

11. Smythe, D.L., "Hole and Electron Mobility in Semiconductors With Large Numbers of Excess Carriers", Ph.D. Thesis, Dept. of Electrical Engineering, MIT, February 1967.

12. Haus, H.A., and Penhune, J., Case Studies in Electromagnetism, Wiley, 1960, pp.259-271.

(References Continued...)

13. Trumbore, F.A., "Solid Solubilities of Impurity Elements in Germanium and Silicon", B.S.T.J., Vol 39, pp.205, January 1960.

14. Przybylski, J. and Roberts, G.N., "The Design and Construction of Tunnel Diodes", Journal Brit. IRE, Vol 22, p.497, December 1961.

15. Navon, D.H., Private Discussion.

16. Taylor, G.R., "Experimental Study of a Germanium Photovoltaic Energy Converter", M.S. Thesis, Dept. of Electrical Engineering, MIT, May 1965.

17. Kennedy, J.T., "Electronic Applications of Sapphire", Vol 8, Electronic Products, August 1965.